Topology optimization of acoustic-structure interaction problems using a mixed finite element formulation

Yoon, Gil Ho; Jensen, Jens Stissing; Sigmund, Ole

Topology Optimization of Acoustic-Structure Interaction Problems using a Mixed Finite Element Formulation

Gil Ho Yoon, Jakob Søndergaard Jensen, Ole Sigmund*

SUMMARY

The paper presents a gradient based topology optimization formulation that allows to solve acoustic-structure (vibro-acoustic) interaction problems without explicit boundary interface representation. In acoustic-structure interaction problems, the pressure and displacement fields are governed by Helmholtz equation and the elasticity equation, respectively. Normally, the two separate fields are coupled by surface-coupling integrals, however, such a formulation does not allow for free material re-distribution in connection with topology optimization schemes since the boundaries are not explicitly given during the optimization process. In this paper we circumvent the explicit boundary representation by using a mixed finite element formulation with displacements and pressure as primary variables (a $\mathbf{u}/p$-formulation). The Helmholtz equation is obtained as a special case of the mixed formulation for the elastic shear modulus equating zero. Hence, by spatial variation of the mass density, shear and bulk moduli we are able to solve the coupled problem by the mixed formulation. Using this modeling approach, the topology optimization procedure is simply implemented as a standard density approach. Several two-dimensional acoustic-structure problems are optimized in order to verify the proposed method.

KEY WORDS: Topology Optimization; Mixed Formulation; Acoustic-Structure Interaction

* Correspondence to: Ole Sigmund (sigmund@mek.dtu.dk)
Department of Mechanical Engineering. Solid Mechanics, Nils Koppels Alle, Building 404,
Technical University of Denmark. DK-2800, Kgs. Lyngby, Denmark

1. INTRODUCTION

Since topology optimization was introduced by Bendsøe and Kikuchi [1], the method has been applied to a large range of engineering problems and has become an important engineering tool [2]. Multi-physics problems, where coupled analyses are required, are promising applications due to the inherent difficulties in obtaining good designs intuitively, and thus recently more research has been conducted in this area [2,3,4,5,6]. These applications, however, have mostly been restricted to problems where the multi-physics behavior is limited to the material-part of the design. The problems become much more complex if the governing equations for the "void" regions are different from those of the material regions, as seen for pressure loads [7,8] or electrostatic actuation [9]. The main problem here is to define a parameterization of the interface between the solid and void regions that allows for topology changes. For the same reason, acoustic-structure optimization problems mainly have been treated with shape and topology optimization formulations where the interface is explicitly known, e.g. reinforcement problems such as design of noise reducing stiffeners [10,11, 12,13, 14, and 15]. However, in [13] topology optimization using genetic algorithms, was applied to acoustic-structure interaction problems for minimization of noise levels allowing for the generation of holes.

For a successful application of gradient-based topology optimization to acoustic-structure interaction problems, a major issue needs to be resolved. The difficulty can be understood by noticing that the pressure and the displacements are the primary variables of the acoustic domain and the structural domain, respectively. To make the two different domains interact with each other, the boundary conditions must be accurately imposed. This implies that the position and parameters of the boundary conditions depend on the given topology. The level set method [12,16-21] inherently has a well-described boundary, however, it is at present not clear how to deal with the two different sets of governing equations using the method. To circumvent the problem, we suggest to look at the interface

problem in an alternative way.

Instead of handling the acoustic and structural domains as two separate domains coupled by boundary integrals, we propose to use a mixed displacement and pressure formulation coupled with the standard density approach to topology optimization. This mixed formulation has previously been suggested for efficient and accurate acoustic-structure interaction analysis [22,23,24]. Our idea to use the mixed formulation in connection with topology optimization comes from previous work on topology optimization of pressure loaded structures [7]. Instead of defining separate and distinct equilibrium equations for the two physical domains, we define a mixed displacement/pressure finite element formulation on the whole domain with both displacements and pressure as primary variables. It can be shown that for vanishing shear modulus, the mixed elasticity formulation degenerates to the Helmholtz equation thus the response of the acoustic domain is also modeled correctly using the mixed formulation when proper shape functions are used.

The paper is organized as follows. Section 2 compares the standard and the mixed formulations for acoustic-structure interaction problems. The mixed displacement/pressure formulation is implemented using the commercial software FEMLAB and tested for two-dimensional problems. Section 3 presents the formulation and the material interpolation functions for topology optimization using the mixed finite element formulation. Section 4 presents several examples of topology optimization applied to two-dimensional vibro-acoustic structures. Section 5 concludes the paper.

2. **u**/*p* MIXED FORMULATION FOR THE ACOUSTIC-STRUCTURE INTERACTION PROBLEM

The acoustic and elastic fields in acoustic-structure interaction problems are commonly solved separately and the coupling is obtained through the surface integral of the interfacing boundary conditions [22,23,24]. In structural optimization, this segregated analysis method with the explicit boundary representation has been used for shape optimization of acoustic devices [11,20,25,26,27]. However, this analysis approach is not applicable to topology optimization problems where boundaries are not explicitly defined. Thus, in this paper, instead of separately solving the Helmholtz equation and the linear elasticity equation, we propose to adopt a mixed displacement/pressure (**u**/*p*) finite element formulation, in which displacements as well as pressure are the primal variables.

2.1. Segregated field equations for acoustic-structure interaction problem

Although our topology optimization scheme is based on the mixed formulation, the governing equations for the acoustic and structural domains as well as the coupling boundary conditions [22, 23, 24,28,] will be shortly outlined for comparison.

Governing equation - Helmholtz equation

Assuming harmonically varying pressure, i.e. $\tilde{p}(t) = p\,e^{i\omega t}$, the governing equation for the pressure in an inhomogeneous acoustic medium is the Helmholtz equation

$$\nabla\cdot(\frac{1}{\rho_a}\nabla p) + \frac{\omega^2 p}{\rho_a c_a^2} = 0 \quad , \qquad (k = \frac{\omega}{c_a}) \qquad \text{on } \Omega_a \qquad (1)$$

where p, ρ_a, and c_a are the pressure in the analysis domain Ω_a, the density of the acoustic domain, and the local speed of sound, respectively. The angular frequency and the wave number are denoted by

ω and k, respectively.

The pressure field is obtained by solving the Helmholtz equation with the proper boundary conditions. In this paper, we consider the following four types of boundary conditions:

$$\text{Pressure boundary condition:} \quad p = p_0 \tag{2a}$$

$$\text{Hard wall condition:} \quad \mathbf{n} \cdot \nabla p = 0 \tag{2b}$$

$$\text{Acceleration boundary condition:} \quad \mathbf{n} \cdot \nabla p = a_n \tag{2c}$$

$$\text{Sommerfeld boundary condition:} \quad \mathbf{n} \cdot \nabla p + i \cdot k \cdot p = 2i \cdot k \cdot p_{in} \tag{2d}$$

where $p_0, \mathbf{n}, a_n$, and p_{in} are the pressure input, the outward unit normal to the fluid medium, the input acceleration, and the pressure amplitude of an incoming wave, respectively. To simulate an absorbing boundary condition without reflection, the Sommerfeld boundary condition (2d) is applied with $p_{in} = 0$ [25].

Governing equation - Linear elasticity problem

Time-harmonic linear structural analysis neglecting the body force can be described by Newton's second law:

$$\nabla \cdot \boldsymbol{\sigma} = -\omega^2 \rho_s \mathbf{u} \qquad \text{on } \Omega_s \tag{3}$$

where $\boldsymbol{\sigma}, \rho_s$, and $\mathbf{u}$ are the stress tensor in the structural domain Ω_s, the structural mass density, and the displacement vector, respectively.

Neumann and Dirichlet boundary conditions are applied as follows:

$$\text{Neumann boundary condition:} \quad \mathbf{n}_s \cdot \boldsymbol{\sigma} = \mathbf{f}^{S_f} \qquad \text{on} \qquad S_f \tag{4a}$$

$$\text{Dirichlet boundary condition:} \quad \mathbf{u} = \mathbf{u}^{S_u} \qquad \text{on} \qquad S_u \qquad (4b)$$

where $\mathbf{f}^{S_f}$ and $\mathbf{u}^{S_u}$ are the surface traction on S_f, and the prescribed displacements on S_u, respectively. The outward unit normal to the solid medium is denoted by $\mathbf{n}_s$.

Analysis method to couple acoustics and structure

If the radiating or scattering structure consists of an elastic material, as shown in Figure 1, then the interaction between the body and the surrounding fluid must be considered [23]. In the multi-physics coupling analysis, the acoustic analysis provides sound pressure to the structural analysis, and the structural analysis provides accelerations to the acoustic analysis.

The interfacing boundary conditions between the acoustic domain and the structural domain can be derived from the continuum equation of the fluid (or air), which actually moves due to the acoustic pressure. For the acoustic domain, the local balance of linear momentum equation should be satisfied as follows:

$$\text{Interface condition for the acoustic domain:} \quad \mathbf{n} \cdot \nabla p = \omega^2 \rho_a \mathbf{n}^{\mathrm{T}} \mathbf{u} \quad \text{in} \quad S_{int} \qquad (5)$$

where S_{int} is the interfacing boundary.

At the interface of the structural domain, the traction of the solid part should equal the pressure. Thus, the following condition should be imposed.

$$\text{Interface condition for the solid part:} \quad \mathbf{f}^{S_{int}} = \mathbf{n} \cdot p \quad \text{on} \quad S_{int} \qquad (6)$$

After imposing the interface boundary conditions of equation (5) and equation (6), the scattering wave and the structural response can be obtained by a standard finite element procedure [13].
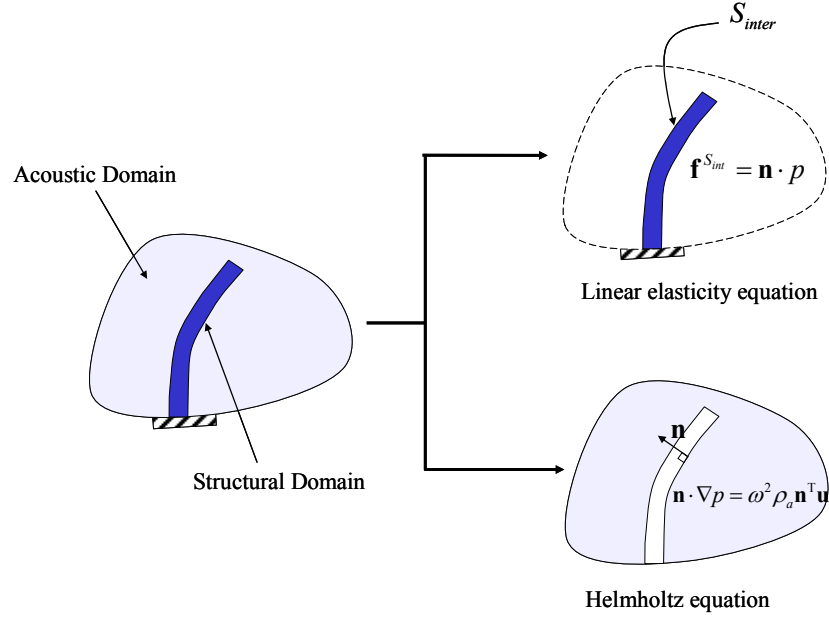
Figure 1. Interaction boundary conditions between acoustic and structural domains.

This procedure has been widely used to calculate responses of acoustic-structure interaction problems [23]. For the procedure, the interfacing boundaries should be exactly or at least approximately defined with parametric curves such as splines, which, for optimization, can be controlled by design variables [8, 29]. Thus, shape optimization has become a natural choice with this analysis procedure [10,12,17,18,19,20,21,25,26,30]. However, in topology optimization the design variables are normally the local material densities. This means that no predefined boundaries exist. Conclusively, although a segregated acoustic-structure analysis method is suitable for calculating responses, the requirements of this method make it difficult to use in topology optimization.

2.2. A mixed finite element formulation for acoustic-structure interaction problems

Topology optimization of acoustic-structural interaction is possible with an explicit boundary representation if one uses discrete variables and thus well-described boundaries (c.f. a genetic algorithm approach [13]). However, in order to reduce computational time and increase mesh resolution it is

desirable to use math-programming algorithms for the solution of the optimization problem and therefore we need continuous design variables. Hence, we propose a simpler method without the need for explicit boundary representation. The method is based on density based material interpolation schemes, by adopting a mixed displacement/pressure finite element procedure [7,22].

In the mixed finite element procedure, the pressure variable is added as an additional primary variable. This mixed displacement/pressure method has been addressed in many books and papers and has especially been used for incompressible or the nearly incompressible elastic media and acoustic-structure interaction problems [22,24,28]. In [7], a mixed formulation was used to solve topology optimization problems with pressure loads, however, to our knowledge, this paper is the first to employ the mixed displacement/pressure formulation for topology optimization of acoustic-structure interaction problems.

Basic principles of the mixed finite element formulation

In the mixed finite element formulation, the governing equations without body forces are:

$$\text{Frequency dependent equilibrium equation:} \quad \nabla \cdot \boldsymbol{\sigma} = -\omega^2 \rho \mathbf{u} \quad \text{on} \quad \Omega \tag{7}$$

$$\text{Stress-strain relationship:} \quad \boldsymbol{\sigma} = K \varepsilon_{\mathrm{v}} \boldsymbol{\delta} + 2G \mathbf{e} \tag{8}$$

$$\text{Pressure and volumetric strain relationship:} \quad p = -K\varepsilon_{\mathrm{v}} \tag{9}$$

$$\text{Deviatoric strain:} \quad \mathbf{e} = \boldsymbol{\varepsilon} - \frac{\varepsilon_{\mathrm{v}}}{3}\boldsymbol{\delta} \quad \text{(3D)} \quad \text{or} \quad \mathbf{e} = \boldsymbol{\varepsilon} - \frac{\varepsilon_{\mathrm{v}}}{2}\boldsymbol{\delta} \quad \text{(2D)} \tag{10}$$

$$\text{Volumetric strain:} \quad \varepsilon_{\mathrm{v}} = \frac{\Delta V}{V} = \varepsilon_{kk} \tag{11}$$

where K, G and ρ are the bulk modulus, the shear modulus and the mass density in the analysis domain Ω, respectively, and δ is Kronecker's delta. The strain tensor is denoted by ε in equation (10).

The bulk and shear moduli are defined as follows:

$$K = \frac{E}{3(1-2\nu)}, \quad G = \frac{E}{2(1+\nu)} \quad \text{(3D)} \tag{12a}$$

$$K = \frac{E}{2(1+\nu)(1-2\nu)}, \quad G = \frac{E}{2(1+\nu)} \text{ (2D-Plane strain)} \tag{12b}$$

$$K = \frac{E}{2(1-\nu)}, \quad G = \frac{E}{2(1+\nu)} \quad \text{(2D-Plane stress)} \tag{12c}$$

where E, and ν are the Young's modulus and the Poisson's ratio, respectively.

The basic approach of mixed displacement/pressure finite element formulations is to interpolate the displacements and the pressure, simultaneously. This requires that we express the principle of virtual work in terms of the independent variables **u** and p:

$$\int_\Omega \delta \mathbf{e}^{\mathrm{T}} \mathbf{C}^{'} \mathbf{e} \, d\Omega - \int_\Omega p \, \delta\varepsilon_{\mathrm{V}} \, d\Omega = \int_\Omega -\omega^2 \rho \, \delta\mathbf{u}^{\mathrm{T}} \mathbf{u} \, d\Omega \tag{13}$$

$$\int_\Omega (p/K + \varepsilon_{\mathrm{V}}) \delta p \, d\Omega = 0 \tag{14}$$

where the virtual displacement, the virtual deviatoric strain and the virtual strain are denoted by $\delta\mathbf{u}$, $\delta\mathbf{e}$, and $\delta\boldsymbol{\varepsilon}$, respectively, $\mathbf{C}^{'}$ is the stress-strain matrix for the deviatoric stress and strain component satisfying the following equation.

$$(\boldsymbol{\sigma} + p\boldsymbol{\delta}) = \mathbf{C}^{'}(\boldsymbol{\varepsilon} - \tfrac{1}{3}\varepsilon_{\mathrm{V}}\boldsymbol{\delta}) \quad \text{(3D)} \quad \text{or} \quad (\boldsymbol{\sigma} + p\boldsymbol{\delta}) = \mathbf{C}^{'}(\boldsymbol{\varepsilon} - \tfrac{1}{2}\varepsilon_{\mathrm{V}}\boldsymbol{\delta}) \quad \text{(2D)} \tag{15}$$

The three involved material properties, the bulk modulus, K, the shear modulus, G, and the mass density

ρ can be used to alternate between the acoustic and the structural domains. For instance, if the analysis domain Ω is assumed to be divided into a structural domain Ω_s and an acoustic domain Ω_a, the three material properties are specified as follows:

$$\Omega = \Omega_s \bigcup \Omega_a, \quad \Omega_s \bigcap \Omega_a = 0 \tag{16}$$

$$\text{Structural domain:} \quad K \equiv K_s, \ G \equiv G_s, \ \rho \equiv \rho_s \quad \text{on } \Omega_s \tag{17}$$

$$\text{Acoustic domain:} \quad K \equiv K_a, \ G \equiv G_a = 0, \ \rho \equiv \rho_a \quad \text{on } \Omega_a \tag{18}$$

where the subscripts 's' and 'a' denote structural and acoustic, respectively.

The mixed finite element implementation of equations (13) and (14) has been used for incompressible media [22,24,28]. Recently, it has also been demonstrated that by varying the shear modulus G and the bulk modulus K, the acoustic domain and the structural domain can be described simultaneously [22, 23, 28]; see Table 1 or reference [7]. Compared to a segregated analysis procedure, a disadvantage of the mixed displacement/pressure formulation is the increased system size due to the additional primary variables, which is significant especially for three dimensional problems.

Table 1. The various analysis types depending on the bulk and the shear moduli.

Category		K (Bulk Modulus)	G (Shear Modulus)
Solid Media	Compressible elasticity	$K > 0$	$G > 0$
	Almost incompressible elasticity	$K \gg G$	
	Incompressible elasticity	Infinite	
Fluid Media	Compressible inviscid fluid	$K > 0$	$G = 0$
	Incompressible inviscid fluid	Infinite	
	Air	Small	

The derivation of the wave equation from the mixed displacement/pressure formulation

The mixed analysis procedure for a linear solid medium is well understood. We will now show that the Helmholtz equation indeed can be derived from the mixed displacement/pressure formulation by assigning the appropriate material properties.

If we set the shear modulus in the acoustic domain Ω_a equal to zero:

$$K \equiv K_a, \;\; G \equiv G_a = 0, \;\; \rho \equiv \rho_a \tag{19}$$

Then the governing (7) and constitutive equation (9) can be simplified as follows:

$$\nabla p - \omega^2 \rho_a \mathbf{u} = 0 \tag{20}$$

$$\nabla \cdot \mathbf{u} + \frac{p}{K_a} = 0 \tag{21}$$

Actually, equations (20) and (21) correspond to *the linearized Euler equation* and *the linear continuity equation*, respectively, which provide the basis for the derivation of the linear wave equation (see chapter 5 in the reference [31]). Substituting the displacement in (20) into equation (21), the Helmholtz equation can be re-derived:

$$\nabla \cdot (\frac{1}{\rho_a} \nabla p) + \frac{\omega^2}{K_a} p = 0 \quad (\text{with } K_a = \rho_a \, c_a^2) \tag{22}$$

Having shown that the Helmholtz equation is contained in the elasticity equations for $G_a = 0$, the remaining issues are the finite element implementation and the boundary conditions. When solving the mixed variational formulations – equations (13) and (14) - a proper finite element implementation must fulfill the so called Inf-sup condition [28] and the boundary conditions. In this paper, we use triangular or quadrilateral elements with second and first order Lagrangian shape functions (T6/3 or Q9/4) for the

displacements and the pressure variables, respectively [22,28]. For the structural domain, implementation of the boundary conditions is straightforward, but some care should be taken in order for the mixed finite element procedure to provide the correct solutions to the Helmholtz equation. In this paper, the boundary conditions shown in Figure 2 have been implemented and tested.
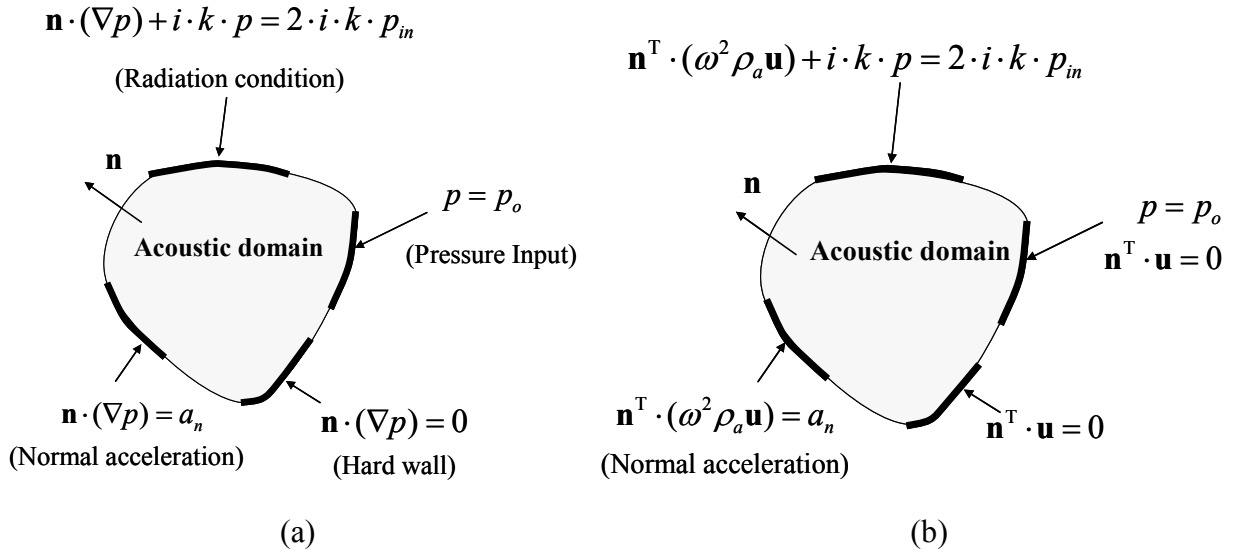

$$\mathbf{n} \cdot (\nabla p) + i \cdot k \cdot p = 2 \cdot i \cdot k \cdot p_{in}$$
(Radiation condition)

n

Acoustic domain

$p = p_o$
(Pressure Input)

$$\mathbf{n} \cdot (\nabla p) = a_n$$
(Normal acceleration)

$$\mathbf{n} \cdot (\nabla p) = 0$$
(Hard wall)

$$\mathbf{n}^{\mathrm{T}} \cdot (\omega^2 \rho_a \mathbf{u}) + i \cdot k \cdot p = 2 \cdot i \cdot k \cdot p_{in}$$

n

Acoustic domain

$p = p_o$
$\mathbf{n}^{\mathrm{T}} \cdot \mathbf{u} = 0$

$$\mathbf{n}^{\mathrm{T}} \cdot (\omega^2 \rho_a \mathbf{u}) = a_n$$
(Normal acceleration)

$$\mathbf{n}^{\mathrm{T}} \cdot \mathbf{u} = 0$$

(a)   (b)

Figure 2. Boundary conditions. (a) Boundary conditions for the Helmholtz equation and (b) the implemented boundary conditions for the mixed finite element method.

Numerical test of the mixed displacement/pressure formulation

In order to verify the model we analyze a number of test problems.

Analysis example 1: Pressure calculation by the mixed finite element formulation

The first analysis example, is the simple acoustic wave problem shown in Figure 3(a). It is solved by the Helmholtz equation as well as by the mixed finite element formulation with the same discretization. Figure 3(b) shows the pressure distribution along the line AA´ computed with the two methods. The small discrepancy is due to the element interpolation order. The mixed formulation uses second and first order interpolations for the displacements and pressure, respectively, whereas second order elements are

used for the pure pressure Helmholtz equation. The discrepancy thus disappears with mesh-refinement.

(a)

(b)

Pressure calculation by
Helmholtz equation

(c)

Pressure calculation by the
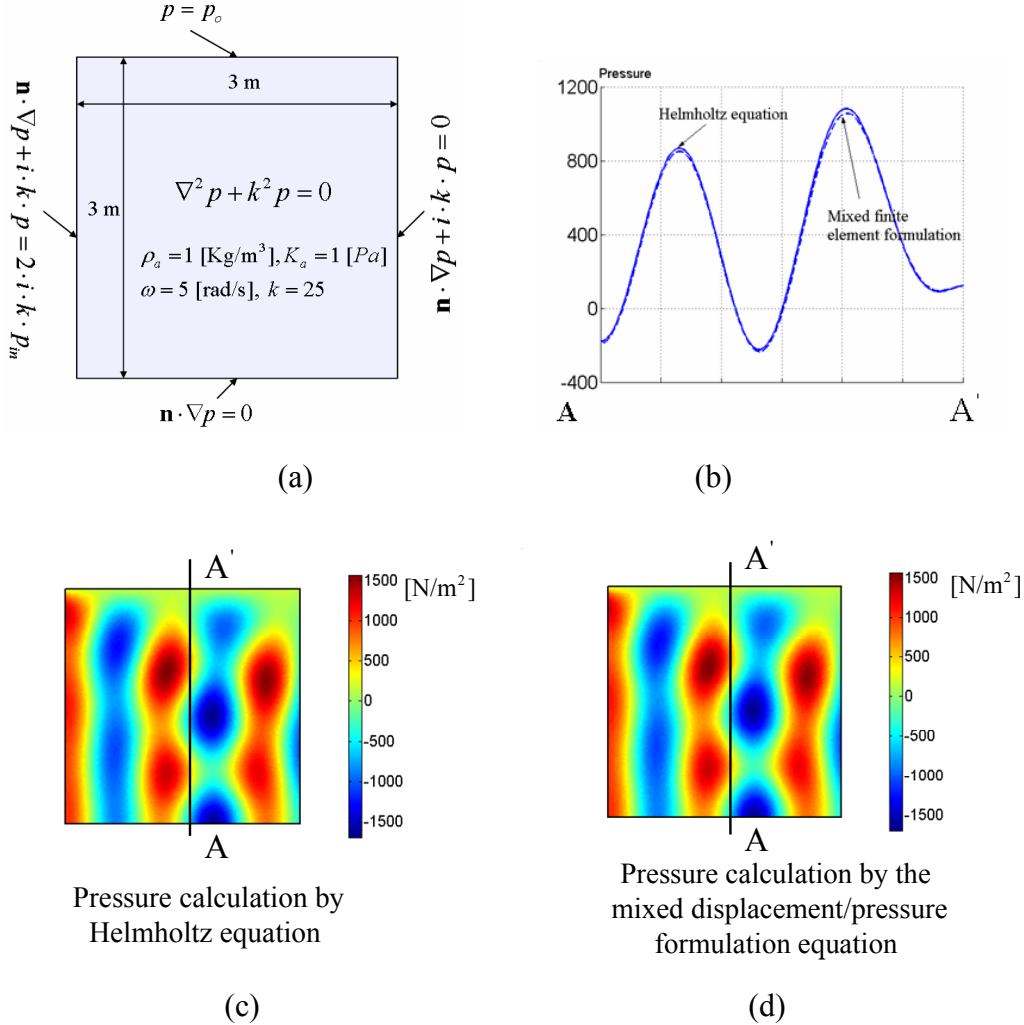mixed displacement/pressure
formulation equation

(d)

Figure 3. Analysis example 1: Acoustic domain analysis with the mixed formulation with various boundary conditions. (a) Problem definition (where $p_0 = 123$ Pa, and $p_{in} = 1000$ Pa), (b) the pressure distribution along AA′, (c) the pressure distribution with the Helmholtz equation, and (d) the pressure distribution with the mixed finite element method.

Analysis example 2: Eigenfrequency analysis

In this example, eigenfrequencies of an acoustic enclosure (Figure 4) are computed. Figure 4(a) and Figure 4(b) show the modeling domain and the boundary conditions applied for the Helmholtz equation and the mixed formulation, respectively. As seen from Table 2, the frequencies are accurately computed

13

using both methods (first 4 frequencies given). We now repeat the computations with the mixed formulation, but replace the hard wall boundary conditions ($\mathbf{n} \cdot \nabla p = 0$) with a massless but very stiff solid region. The computed eigenfrequencies are now seen to deviate slightly from the analytical values. The reason for this discrepancy can be seen from the computed mode shape seen in Figure 4(c), where the close-up plot reveals a boundary layer in the vicinity of the solid-acoustic boundary. Thus the boundary introduces a no-slip condition, which is not modeled by the ordinary Helmholtz equation. This no-slip condition cannot be circumvented in the present topology optimization model but its effect is diminished with mesh-refinement. It may, however, be discussed whether the idealized Helmholtz equation actually represents acoustic vibrations accurately. In reality, the physical boundary condition is no-slip and therefore there will always be a small boundary layer in an exact model of an acoustic problem.
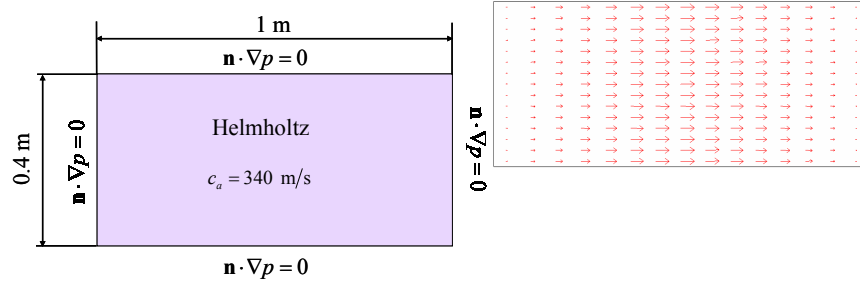
Problem definition   The first mode shape (pressure)

(a) Helmholtz equation
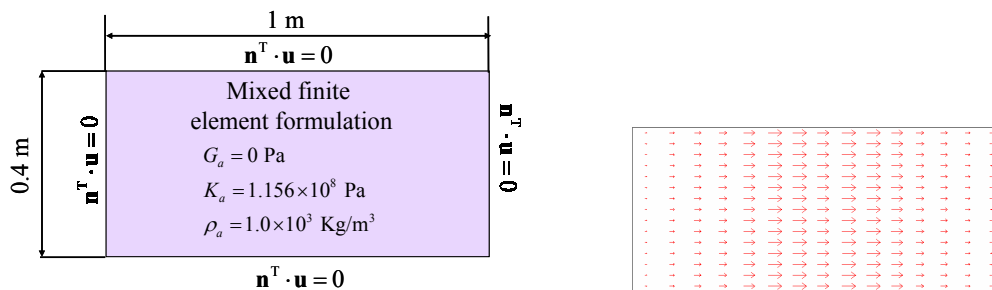
Problem definition   The first mode shape (pressure)

(b) Mixed finite element formulation without the elastic foundation

Problem definition	The first mode shape (pressure)
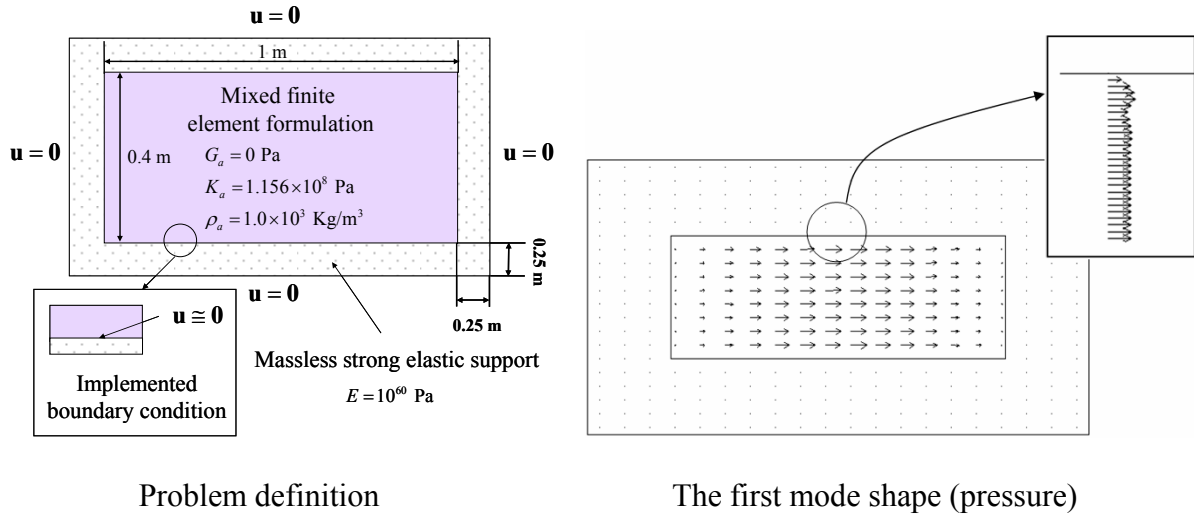
(c) Mixed finite element formulation with the stiff elastic foundation

Figure 4. Analysis example 2: Eigenfrequency analysis using Helmholtz equation and the mixed formulation without and with the stiff elastic foundation.

Table 2. The comparison of the eigenfrequencies for the models shown in Figure 4.

Order	Helmholtz Figure 4(a)	Mixed formulation Figure 4(b)	Mixed formulation Figure 4(c)	Analytical Frequency in Ref. [24]
1	170.82 Hz	170.00 Hz	168.64 Hz	170.0 Hz
2	340.87 Hz	340.55 Hz	337.50 Hz	340.0 Hz
3	425.36 Hz	425.04 Hz	423.98 Hz	425.0 Hz
4	456.89 Hz	457.79 Hz	454.70 Hz	457.7 Hz

Analysis Example 3: A two-dimensional fluid-structure interaction problem

A simple two-dimensional acoustic-structure problem is analyzed using both standard procedure with interface boundary conditions and the mixed formulation. The analysis domain is defined by Figure 5. With the standard finite element method, the computed displacement at the interface between the solid

and the acoustic domains match analytical results obtained for an identical 1D system. However, small discrepancies appear for the mixed formulation. The reason is that continuous shape functions are used for the displacements and the pressure at the interface boundary, whereas the standard displacement finite element procedure use discontinuous shape functions in the interface boundary. Again, the discrepancies diminishes with mesh-refinement.
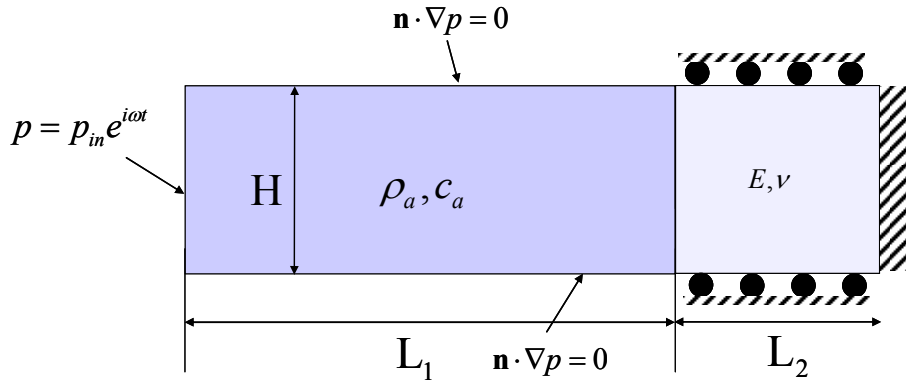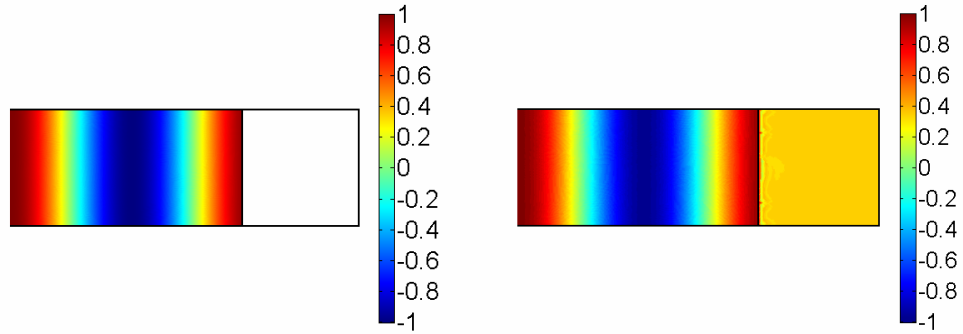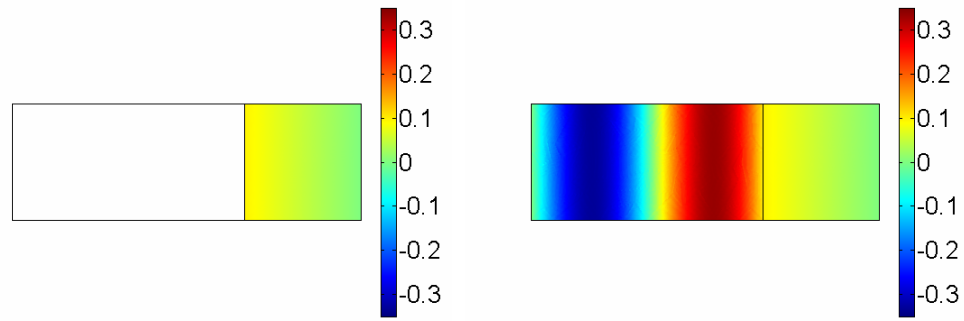

Figure 5. Two-dimensional acoustic-structure test problem.

($L_1 = 2$ m, $L_2 = 1$ m, $H = 1$ m, $E = 10$ N/m^2, $\nu = 0.0$, $\rho_a = 1$ Kg/m^3, $c_a = 1$, $p_{in} = 1$)

(a) The pressure distribution (Left: standard and Right: mixed formulation)

(b) The *x*-displacement (Left: standard and Right: mixed formulation)

Figure 6. Analysis results for the two dimensional acoustic-structure interaction problem in Figure 5 for $\omega=3$ (rad/s).

Table 3. The comparison of the displacements at the position ($x=2$, $y=0.5$) with respect to the different angular speed.

Angular Speed ω [rad/s]	0.001	1	2	3	4
Displacement, 1D analytical model [m]	0.1000	-0.1972	-0.1991	0.0958	-0.1848
Displacement, 2 D standard fem [m]	0.1000	-0.1972	-0.1991	0.0958	-0.1848
Mixed 2D formulation [m]	0.0988	-0.1932	-0.1999	0.0945	-0.1766

3. PARAMETERIZATION METHOD FOR TOPOLOGY OPTIMIZATION

3.1. Parameterization of design variables

For the mixed finite element governing equation to alternate between the Helmholtz equation and the linear elasticity equation, the involved material properties, i.e., the bulk modulus, the shear modulus, and the structural mass density, should be properly interpolated with respect to the design variables according to equations (16-18) [7]. Since we are dealing with vibration problems, it is important that we use an interpolation scheme that has finite stiffness to mass ratio for the design variables approaching zero [32]. This excludes the traditional SIMP interpolation scheme, thus we instead use a two-material RAMP formulation [33]:

$$K(\gamma) = K_s \frac{\gamma}{1+(1-\gamma)n} + K_a \left(1 - \frac{\gamma}{1+(1-\gamma)n} \right) \tag{23a}$$

$$G(\gamma) = G_s \frac{\gamma}{1+(1-\gamma)n} + G_a \left(1 - \frac{\gamma}{1+(1-\gamma)n} \right) = G_s \left(1 - \frac{\gamma}{1+(1-\gamma)n} \right) \tag{23b}$$

$$\rho(\gamma) = \rho_s \gamma + \rho_a (1-\gamma) \tag{23c}$$

$$0 \leq \gamma \leq 1 \tag{23c}$$

where γ is the design variable. The penalty factor for the bulk/shear modulus is denoted by n. In these interpolation functions, the solid media properties are obtained for $\gamma=1$ and the acoustic media properties for $\gamma=0$. Positive values between 3 and 6 are used for n. In [34] the physical realizability of material microstructures with elastic properties corresponding to different interpolation schemes was proven for linear elasticity problems. In the present acoustic-structural formulation the question of physical realizability is not easy to answer since microscopic structural-acoustic response depends on length-scale and excitation frequency, however, it is reasonable to assume that there exist porous media with properties obeying the RAMP interpolation assuming that the microstructural scale is much smaller than the acoustic wave length. Anyway, we are only using the intermediate densities as a means

for using gradient-based methods for the optimization. Whether we use physically realizable intermediate densities or not is not important as long as we end up with solid-void final designs.

3.2. Implementation of the **u**/p mixed finite element formulation

The **u**/p mixed finite element procedure is implemented in the FE-package FEMLAB in a MATLAB environment. The Matlab based script FE-package is useful in implementing the finite element formulation and optimization since it allows easy implementation of different analysis domains and change of element types, etc. as well as for the possibility for semi-automated analytical sensitivity analysis, see [35,36,37].

The topology optimization problem is implemented in the standard way. We use nodal design variables, mesh-independent filtering [2] and the Method of Moving Asymptotes (MMA) for solving the optimization problem [38]. The sensitivity analysis is performed analytically using the adjoint method.

In order to improve convergence and obtain mesh-independent design we use the sensitivity filtering method proposed by Sigmund [33].

4. TOPOLOGY OPTIMIZATION OF ACOUSTIC-STRUCTURE INTERACTION STRUCTURES

In this section, several topology optimization problems for acoustic-structure interaction will be solved using the implemented mixed displacement/pressure (**u**/p) formulation. We start with simpler examples and proceed to more complex ones in order to demonstrate different computational and physical aspects of the method and the solutions.

4.1. Topology optimization for a massless flexible partition

First we optimize a massless partition as illustrated in Figure 7. The rightmost grey domain is supposed to be shielded from an incoming wave from the left. Structural material can be distributed in the central design domain. The full model consists of three domains: the acoustic domain with the incoming wave, the design domain, and another acoustic domain with absorbing boundary conditions. For simplicity, we assume a single excitation frequency.
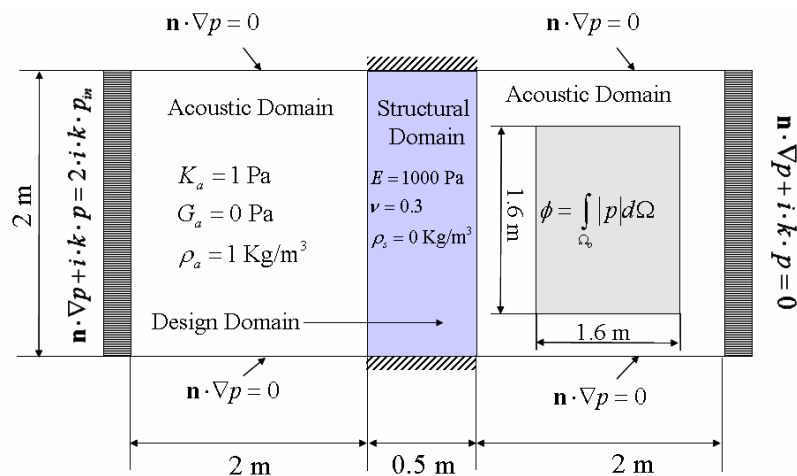
Figure 7. Topology optimization of a massless flexible partition. Definition of the optimization problem including boundary conditions, design domain and objective function. E, ν, and ρ_s are Young's modulus, the Poisson's ratio, and the structural density, respectively. The incoming wave amplitude is p_{in} =1 kPa.

Topology optimization without volume constraint

For structural acoustic design problems constraining structural mass is not necessarily an issue, hence we first approach the design problem without a mass constraint. The objective is to minimize the acoustic pressure in the objective domain (c.f. equation (24)). For a uniform initial design ($\gamma_{initial}$ =0.4) and an excitation frequency of f=1/π (Hz), the solution in Figure 8a is obtained. It is seen that even though a solid wall is forming in the initial steps, the final optimized solution has a fluid-filled cavity. Hence, the optimal volume fraction is a result of the optimization. Since there is no structural resonance, the response curve (Figure 8c) is quite smooth. The small peaks at f=0.5 and 1 (Hz) correspond to acoustic resonances in the left most acoustic domain. For higher excitation frequencies (above 1 Hz), the response curve is less smooth indicating local resonances in the cavity.

$$\underset{\gamma}{\text{Minimize}} \quad \phi = \int_{\Omega_o} |p| \, d\Omega \qquad \text{(the objective domain is defined in } \Omega_o \text{.) (24)}$$
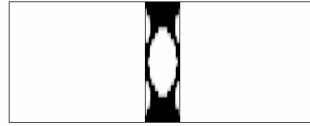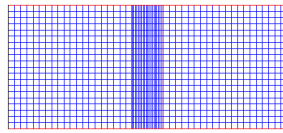
(a) $\phi_{optimized}$ =45.8598N (Mass=58.65%)
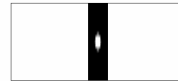
1st iteration   2nd iteration   7th iteration

15th iteration   40th iteration   76th iteration

(b)

(c)
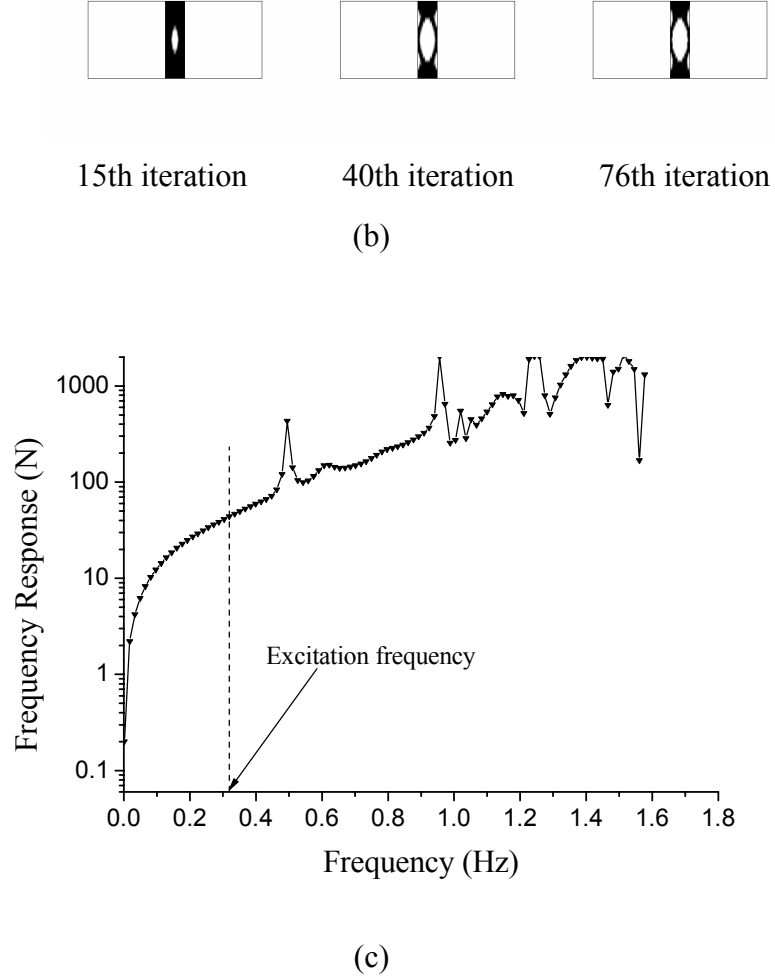
Figure 8. Optimized topology using formulation (24) with excitation frequency $f=1/\pi$ (Hz). (a) Mesh and optimized density distribution, (b) optimization history, and (c) the frequency response where the dashed line indicates the excitation frequency used in the optimization.

Optimization with volume constraint

If we include a volume constraint, the formulation of the optimization problem becomes

$$\underset{\gamma}{\text{Minimize}} \ \phi = \int_{\Omega_o} |p| \, d\Omega \tag{25}$$

$$\text{Subject to} \ \int_{\Omega_o} \gamma \, d\Omega \leq V_0$$

where V_0 is the allowed volume. In this example, we set V_0 equal to 50% of the area of the design

domain. The resulting topology is seen in Figure 9 and it can be seen that it is simply a thinned version

of the free volume solution from Figure 8. Even though convergence to local minima was not observed

for the present example, we recommend to impose a volume fraction constraint in all cases in order to

hinder convergence to local minima.
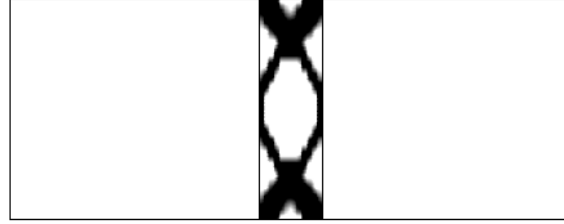
(a) $\phi_{optimized} = 61.384\ N$ (Mass=50.00%)
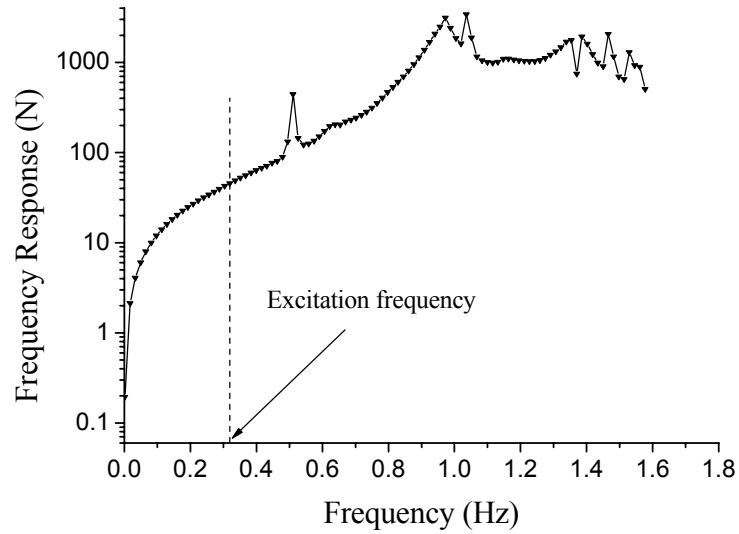
(b)

Figure 9. Optimization results with the volume constraint (50%).

4.2. Topology optimization for flexible partition including structural mass density

In reality, structural mass must be included, however, this makes the optimization problem more

difficult to solve due to problems with local resonances. In this section we use the same problem formulation and design domain as before (equation (25) and Figure 7) but include the effects of mass density.

The initial frequency response of the defined objective function for two different structural mass densities (ρ_s = 11 and 15 Kg/m^3, respectively) and the structure from Figure 7 are shown in Figure 10. Obviously, the fundamental structural eigenfrequency for ρ_s=11 Kg/m^3 is higher than for ρ_s=15 Kg/m^3. Thus, setting the excitation frequency to f=5/2π between the two peaks in Figure 10 and minimizing the objective function, one can expect a widely different behavior for the two values of ρ_s during optimization. In Figure 11 and Figure 12, the optimized structures and the frequency response during some optimization steps are plotted. With the lighter structural density ρ_s=11 Kg/m^3, the fundamental eigenfrequency is pushed upwards. This leads to an optimized structure having a larger fundamental frequency as Figure 11 shows. Oppositely, when the heavier structural density (ρ_s=15 Kg/m^3) is used, the fundamental structural frequency is pushed downwards. Thus, to minimize the objective function, the optimized structure gets a low fundamental frequency. Some observations can be made: First, it can be postulated that similar topologies will be obtained as long as the excitation frequency stays at the same side of the peak. Second: When the excitation frequency is placed to the left of the fundamental frequency and there is no mode switching during optimization, the optimized topologies resemble those found from direct maximization of the fundamental eigenfrequency as seen in Figure 11. Similar observations are reported by Olhoff and Du [15].
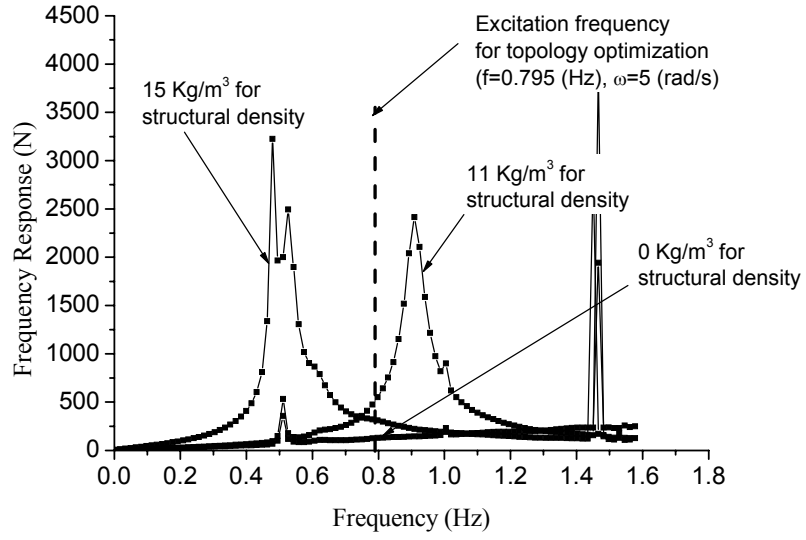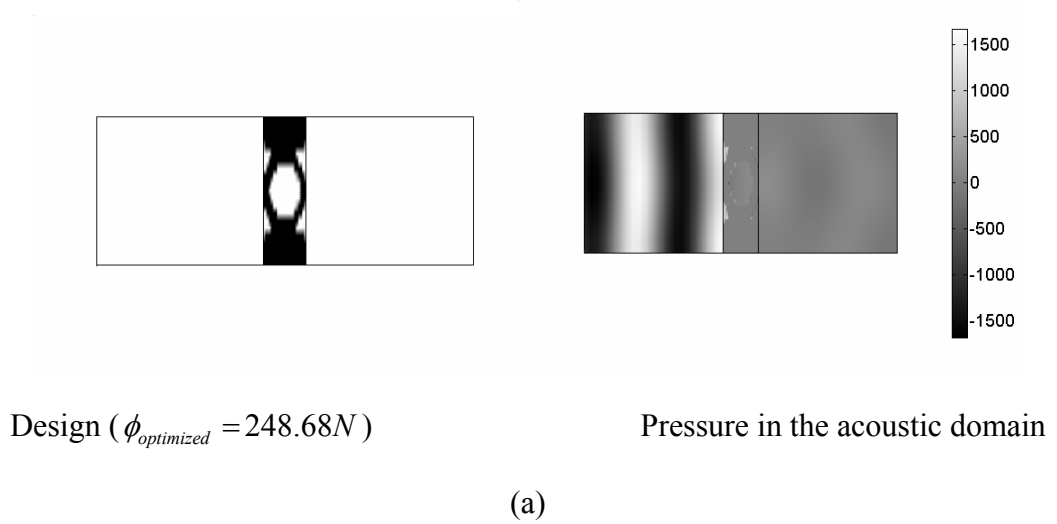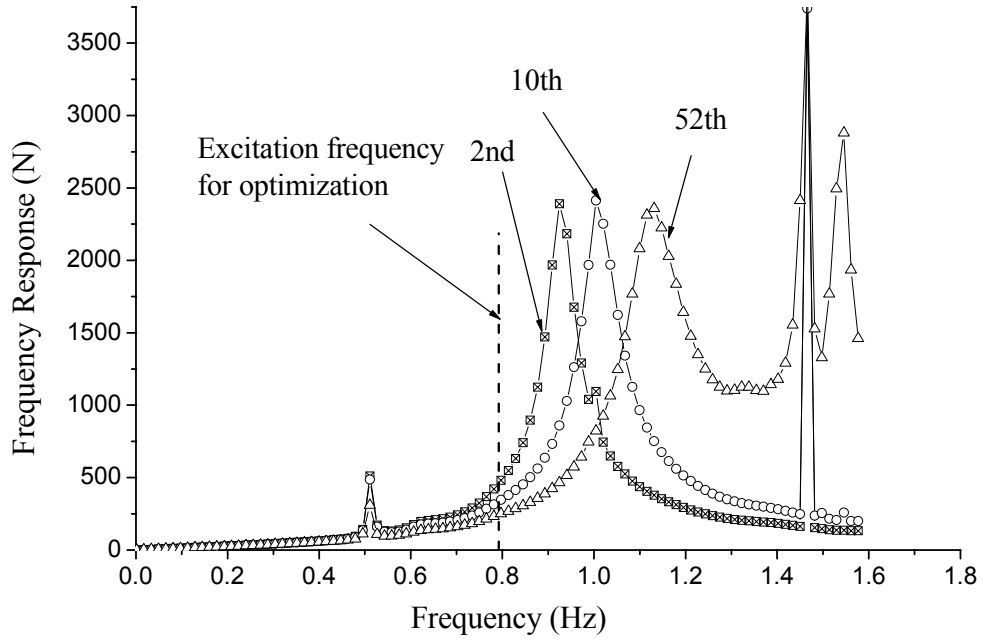
Figure 10. The frequency response of $\phi = \int\limits_{\Omega_o} |p|\, d\Omega$ of Figure 7 with various structural mass densities (the initial design variables are set as $\gamma = 0.5$).
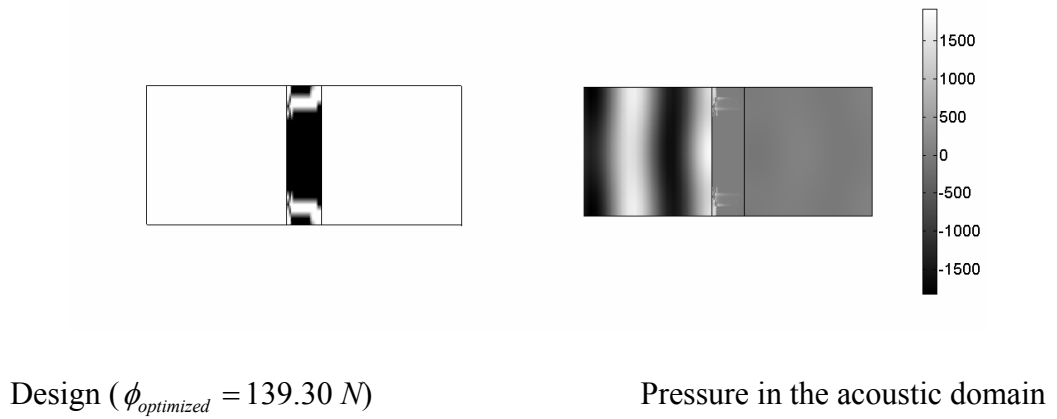
$$\underset{\gamma}{\text{Minimize}} \qquad \phi = \int\limits_{\Omega_o} |p|\, d\Omega \qquad\qquad (26)$$

Design ($\phi_{optimized} = 248.68N$)   Pressure in the acoustic domain

(a)

(b)

Figure 11. Results for $\rho_s = 11 \, Kg/m^3$. (a) Optimized topology, and (b) frequency response during the optimization process.

Design ($\phi_{optimized} = 139.30 \, N$)   Pressure in the acoustic domain

(a)
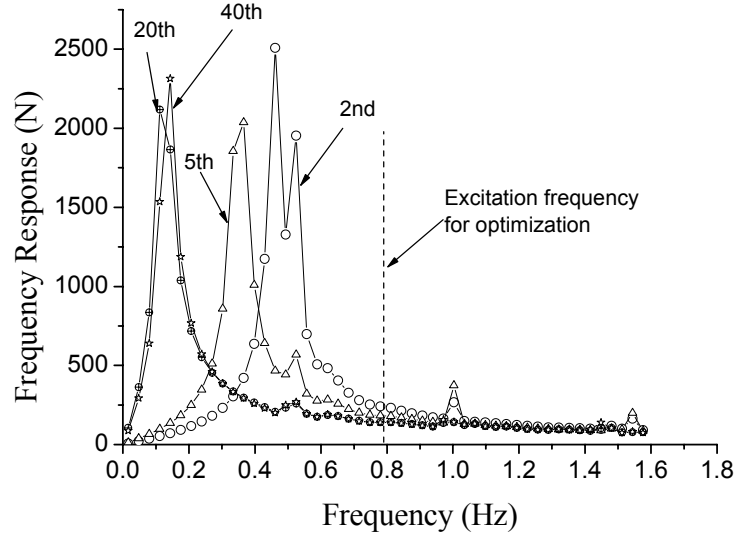
(b)

Figure 12. Result for $\rho_s = 15\,Kg\,/\,m^3$. (a) Optimized topology, and (b) frequency response during the optimization process.

Minimizing the objective function for $\rho_s = 15\,Kg\,/\,m^3$, a topology with very thin parts is obtained as seen in Figure 12. The structure corresponds to a large mass suspended with very soft springs, i.e. a structure with a very low fundamental frequency. Although the objective function is very low, such a structure is not desired from a structural perspective. To overcome this difficulty, the obvious solution would be to impose a constraint on the static response, however, this does not make much sense for an acoustic load. Instead we impose an integral constraint on the response for excitation frequencies below a certain threshold frequency. The modified optimization problem is given in equation (27). The first constraint is the volume constraint. The second constraint confines the optimization results to have a small response in the low frequencies range thus eliminating structurally degenerate designs.

$$\underset{\gamma}{\text{Minimize}}\ \phi = \int\limits_{\Omega_p} |p|\, d\Omega \tag{27}$$

27

Subject to $\int_{\Omega_o} \gamma \, d\Omega \le V_0$

$$\frac{\int_0^{\theta \cdot f^*} \phi df}{\theta \cdot f^*} - \zeta \phi_{f^*} \le 0$$

(where $0 < \theta < 1$ and $0 < \zeta < 1$)

In the new constraint, θ denotes the threshold fraction, ζ denotes the constraint value, f^* is the excitation frequency and the objective function at the excitation frequency is denoted by ϕ_{f^*}. Hence selecting $\theta = 0.5$ and $\zeta = 1/3$, we impose that the average response for frequencies below 50% of the excitation frequency should be less than a third of the response at the excitation frequency. We use 3 point integration for the integral constraint.

Using this formulation we obtain the results presented in Figure 13. It is clearly seen how we obtain a structurally reasonable design and we note that even though the fundamental frequency of the initial design was below the excitation frequency, it shifted to be higher than the excitation frequency for the final design.
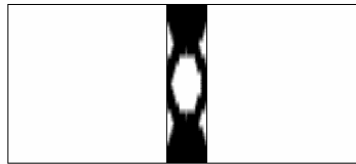
(a) $\phi_{optimized} = 510.43N$
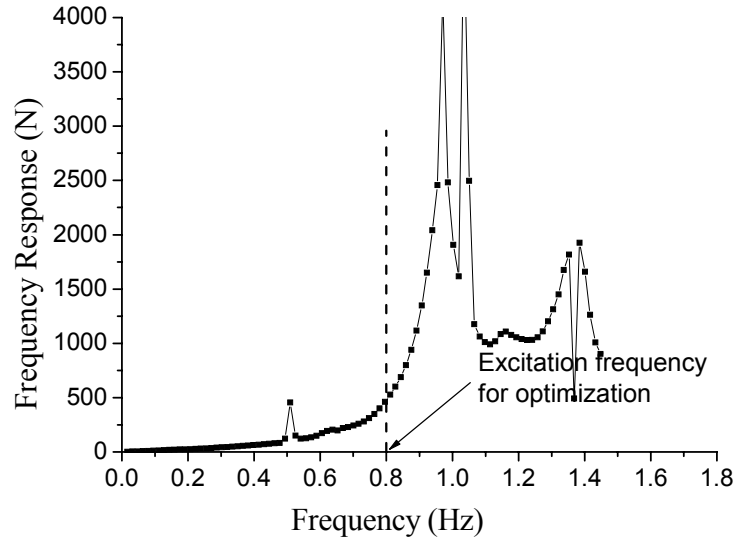
(b)

Figure 13. Results for $\rho_s = 15 \, Kg/m^3$ using the optimization formulation (27) with $\theta = 0.9, \zeta = 0.1$ and 70% mass usage. (a) Optimized topology, and (b) the frequency response.

Instability and local optima

In the topology optimization of acoustic-structure interaction problems, we have observed fluctuation of the objective function represented by the acoustic pressure field, dependency on the initial design and dependency on the excitation frequency. To examine these phenomena in further detail, the frequency responses for the above example with various uniform material distributions are shown in Figure 14. For higher initial uniform density distributions (γ =0.7 and γ =1), the responses are quite smooth and for the former case the response curve is shifted to the left due to the smaller stiffness to mass ratio. Hence, depending on starting guess and excitation frequency we may obtain widely different solutions. For low initial uniform density distributions (γ =0.1), the fundamental structural frequency has shifted even further to the left but we also observe fluctuations in the frequency response corresponding to local modes in the low density structural domain [39]. Here it should be noted that the problem with local modes is much more pronounced when using the SIMP interpolation scheme instead of RAMP. In

fact, the SIMP interpolation scheme turns out to be useless for solving acoustic-structural problems with the present formulation due to the stiffness to mass ratio going to infinity for vanishing density. Despite the superiority of the RAMP approach for solving the present kind of problems, we still experience local mode problems as discussed above. To overcome these, we may use artificial damping, continuation methods for the excitation frequency or other stabilization techniques, which have not been used in this paper. These extensions will be left for future research.
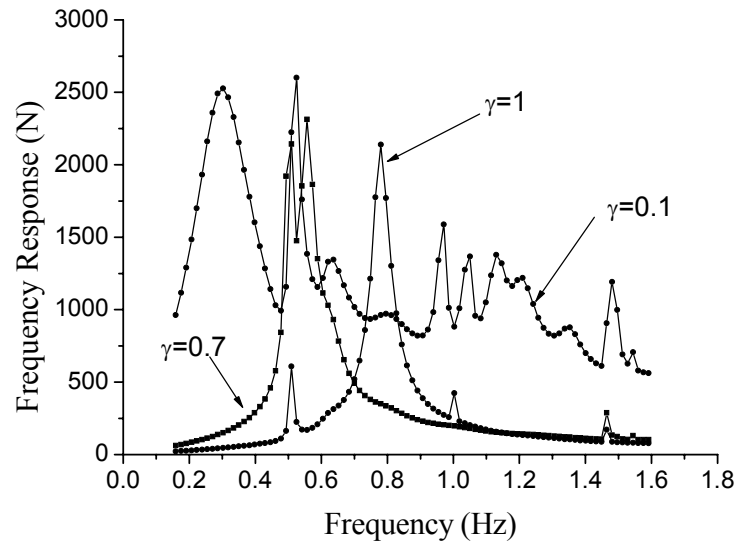
Figure 14. The frequency responses of various uniform design variables.

4.3. Topology optimization for static pressure loading problems

In reference [7], topology optimization for static pressure loads was formulated using a mixed displacement pressure formulation with incompressible fluid regions. In this example, we demonstrate that similar problems can be solved using the present acoustic formulation using low excitation frequencies and compressible fluid regions. The design problem is sketched in Figure 15. Slowly varying acoustic pressure is imposed on all boundaries except for the central part of the bottom edge. A rectangular box is chosen as the objective domain, i.e. a structure should be built around the objective domain in order to shield it from the external acoustic field. The optimized topology is seen in Figure 15(b). The result corresponds almost exactly to those found in the literature [7, 8].
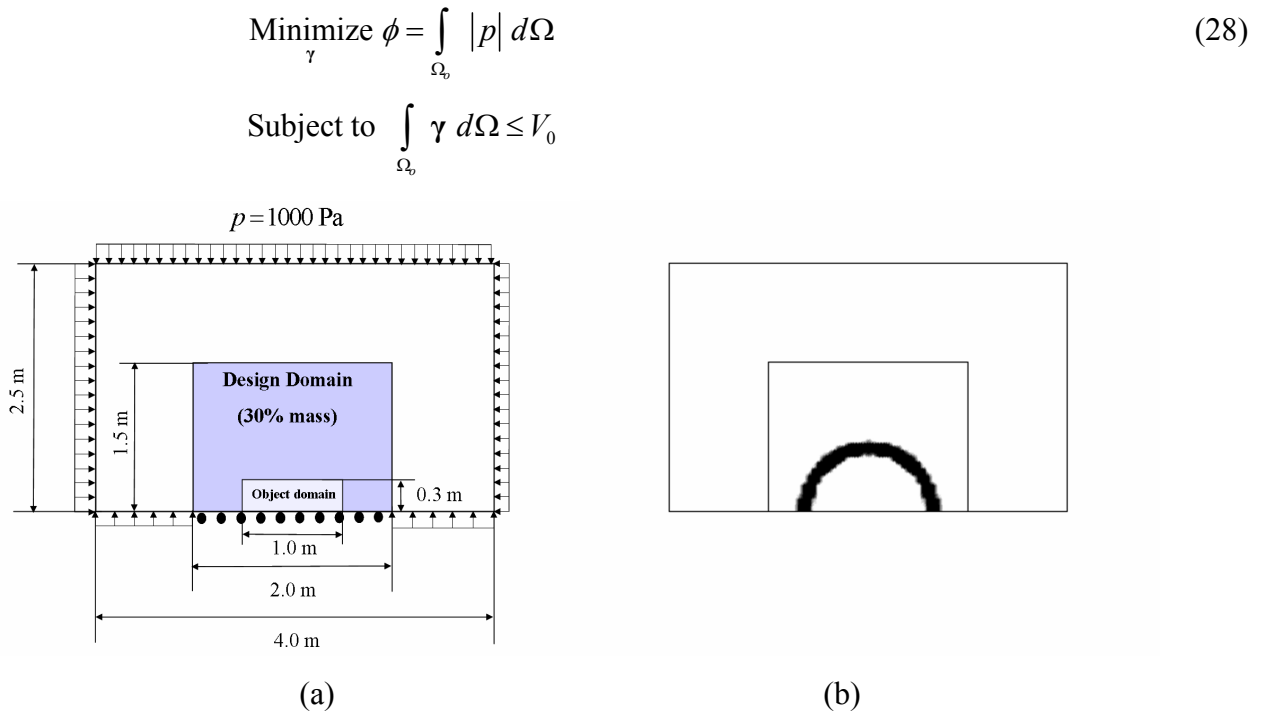
$$\text{Minimize } \phi = \int_{\Omega_o} |p|\, d\Omega \qquad\qquad (28)$$

$$\text{Subject to } \int_{\Omega_o} \gamma\, d\Omega \le V_0$$

(a)　　　　　　　　　　　　(b)

Figure 15. Optimized topology for minimization of pressure intensity. (a) Problem definition (Acoustic properties: $K_a = 1$ Pa, $G_a = 0$, $\rho_a = 1$ $f = \dfrac{1.0 \times 10^{-5}}{2\pi}$ Hz , Structural properties: $E = 1000$ Pa , $\nu = 0.3$, $\rho_s = 1$, Mass: 10%), (b) and optimized topology.

4.4. Topology optimization for vibrating structure

For the last example, we consider a vibrating structure (Figure 16) submerged in two different fluid media. The fluid media are selected with widely different properties, e.g. Mercury and Air, in order to study the effect of the fluid load. The initial responses for the clamped T-shape structure in Figure 16a are shown in Figure 16(b) and (c). It is seen that the fundamental frequency for the Mercury case is much smaller than for air as expected. We want to optimize the topology of the rectangular domain above the T-shape structure in order to minimize the work (or minimize displacement amplitude for fixed force amplitude) of the external force at the bottom of the structure. The optimization problem is formulated as
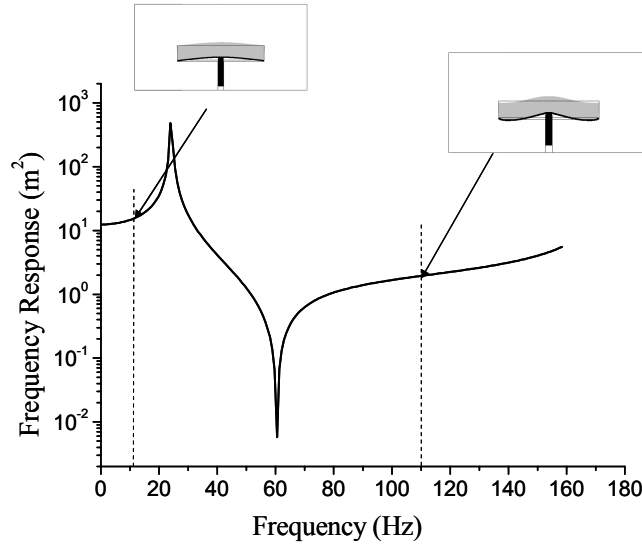
$$\text{Minimize } \phi = \int_{\Gamma_o} |\mathbf{n} \cdot \mathbf{u}| \, d\Gamma \qquad \text{(where the objective boundary is defined by } \Gamma_o.) \quad (29)$$

$$\text{Subject to } \int_{\Omega_o} \gamma \, d\Omega \leq V_0$$

$$\phi = \int_{\Gamma_o} |\mathbf{n} \cdot \mathbf{u}| \, d\Gamma$$

(a)

32
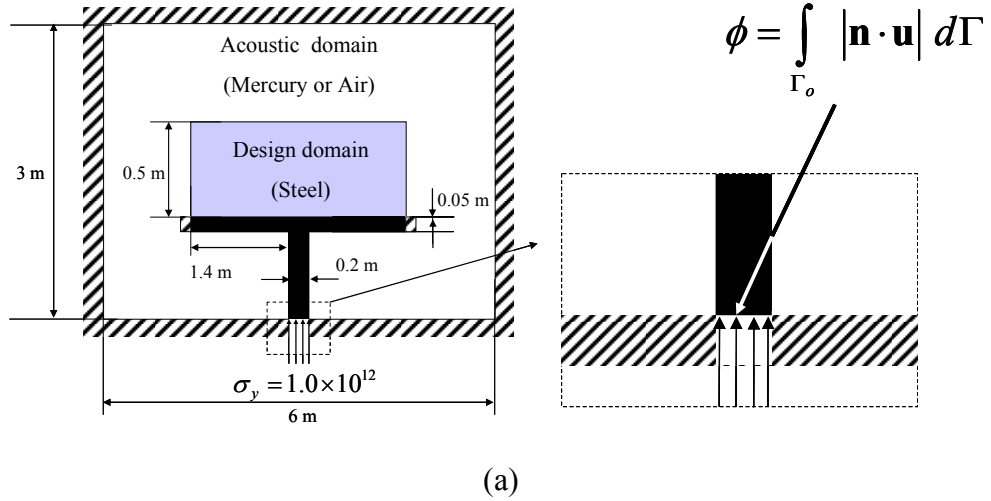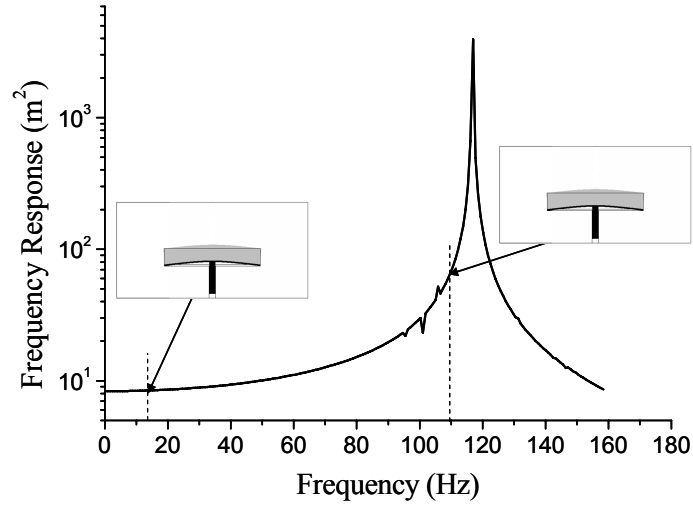
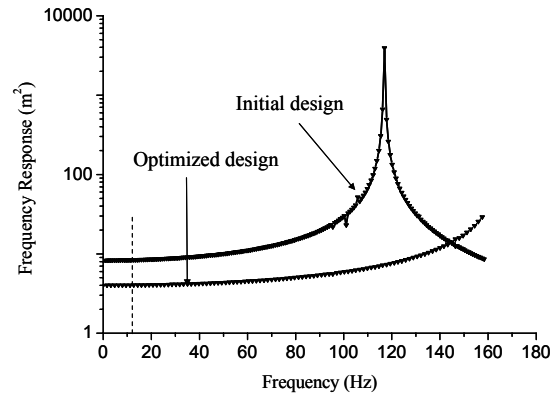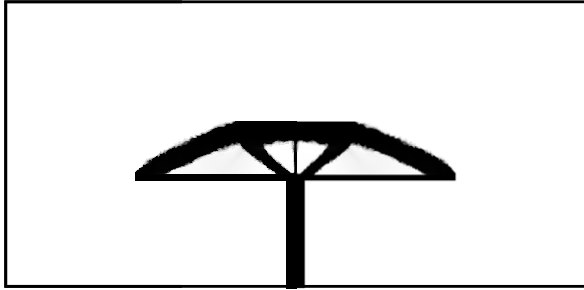(b) Steel and air

(c)   Steel and Mercury

Figure 16. Optimization problem definition for harmonic loading. (a) Problem definition (bulk modulus of steel: $200\,GPa$, mass density of steel: $7700\ Kg/m^3$, bulk modulus of air: $1.01325\times10^6\,Pa$, mass density of air: $1.293\,Kg/m^3$, bulk modulus of Mercury: $25.3\,GPa$, mass density of Mercury: $13600\,Kg/m^3$, mass percentage: 50%), (b) frequency response for steel and air, and (c)   frequency response for steel and Mercury.

For the numerical tests, we consider the excitation frequencies $f = \dfrac{100}{2\pi}$ (Hz) and $\dfrac{700}{2\pi}$ (Hz). When Air is

used as fluid medium, its influence on the T-shape structure is negligible compared to Mercury and both excitation frequencies are located on the left side of the fundamental frequency. Therefore, the first eigenfrequency is maximized for the resulting topologies as seen in Figure 17b and c. It is also observed that the optimized topologies are very similar to the one obtained for minimizing the compliance (Figure 17a).
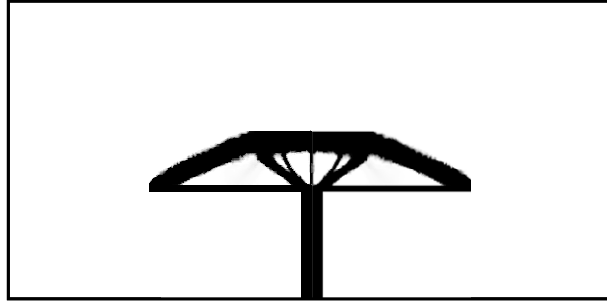
(a)

(b) $\phi_{optimized} = 4.038\ m\ (f = \dfrac{100}{2\pi}\,\mathrm{Hz})$
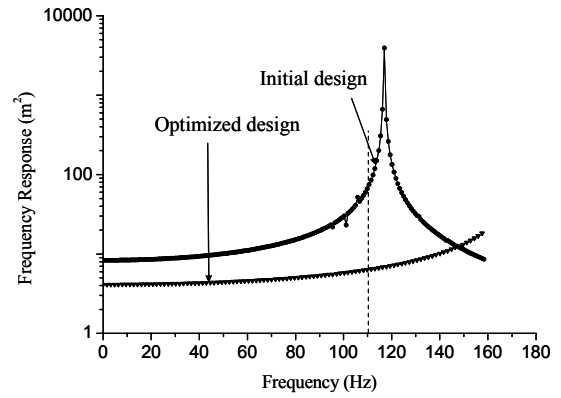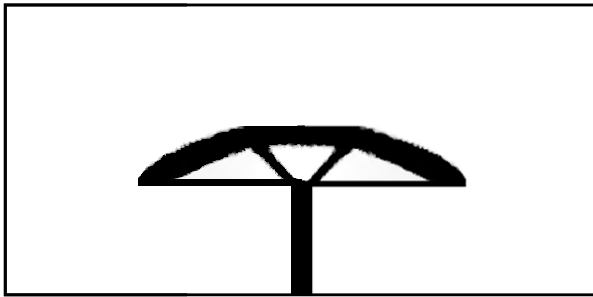
(c) $\phi_{optimized} = 6.453\ m\quad (f = \dfrac{700}{2\pi}\,\mathrm{Hz})$

Figure 17. Results for steel and air. (a) Optimized topology for compliance minimization, (b) optimized topology for $f = \dfrac{100}{2\pi}\,\mathrm{Hz}$, and (c) optimized topology for $f = \dfrac{700}{2\pi}\,\mathrm{Hz}$.

When the room is filled with Mercury, the T-shape structure has a left shifted frequency response compared to the air filled room. The first excitation frequency ($f = \dfrac{100}{2\pi}$ Hz) is located to the left of the first eigenfrequency. However, the second excitation frequency ($f = \dfrac{700}{2\pi}$ Hz) is located to the right of the first eigenfrequency and the antinode. Therefore, we get different resulting topologies for the two excitation frequencies as seen in Figure 18a and b. In the latter case it is interesting to see how the optimized topology has two dome like structures indicating the pressure nature of the loading. The dome like designs are not seen for the former cases since here the loading is dominated by the external force at the lower edge of the design domain and less by the fluid resistance.
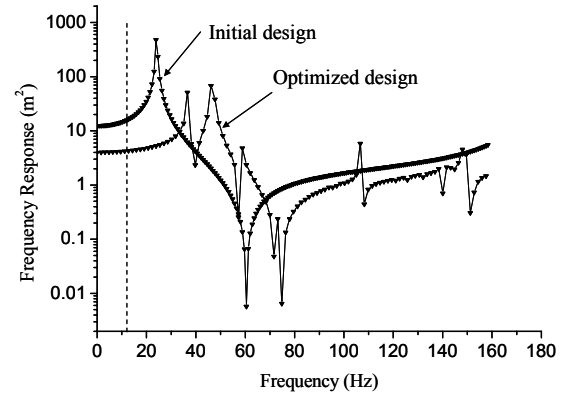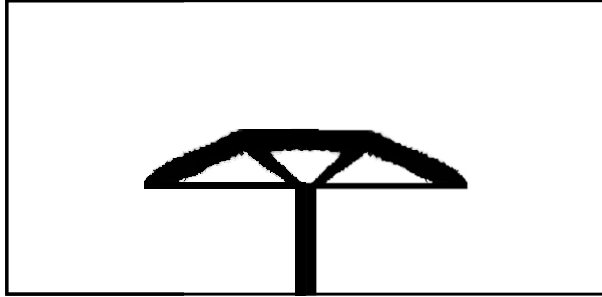
(a) $\phi_{optimized} = 4.460\,m\,(\dfrac{100}{2\pi}\,\text{Hz})$
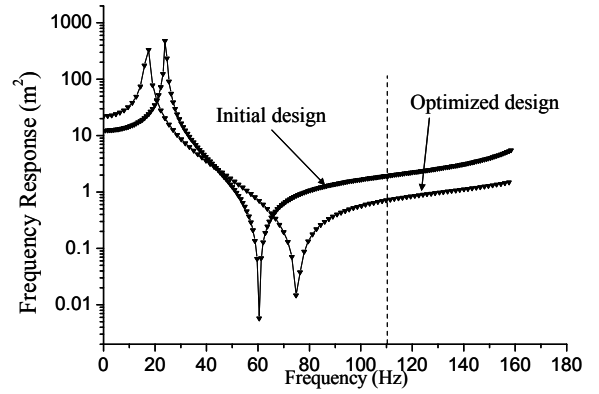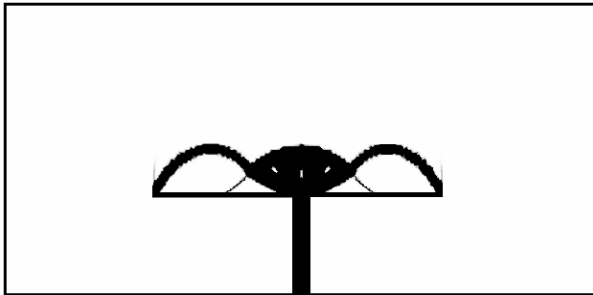
$$\text{(b)} \quad \phi_{optimized} = 0.736 \, m \, (\frac{700}{2\pi} \text{Hz})$$

Figure 18. Results for steel and Mercury. (a) Optimized topology for $\frac{100}{2\pi}$ Hz, (b) optimized topology for $\frac{700}{2\pi}$ Hz.

5. CONCLUSION

In this paper we have proposed a new formulation for topology optimization of acoustic-structural problems. The method is based on a mixed pressure-displacement finite element formulation that circumvents explicit formulation of the boundary conditions between fluid and structure. The interpolation between fluid and structure is modeled using the RAMP scheme that preserves a finite stiffness to mass ratio when the design variables (structural densities) approach zero.

The efficiency of the method is demonstrated by several examples. The optimized designs may converge to different local minima depending on initial material distribution and excitation frequencies. Also depending on the material properties of the fluid medium and the excitation frequency, the optimized topologies may contain features such as dome like shapes known from pressure loaded structural design problems.

In future work we will address issues like fluctuating responses due to local modes, optimization over wider frequency intervals, extensions to 3d and the modeling of the non-structural domains by pure (pressure) Helmholtz formulation in order to save CPU-time.

6. ACKNOWLEDGEMENTS

37

REFERENCES

1. Bendsøe MP, Kikuchi N. Generating optimal topologies in structural design using a homogenization method. *Comp. Meth. Appl. Mech. Engng.* 1988; **71**:197-224.

2. Bendsøe MP, Sigmund O. *Topology Optimization Theory, Methods and Applications.* Springer-Verlag: New York, 2003.

3. Sigmund O. Design of Multiphysics Actuators using Topology Optimization – Part I: One Material Structure. *Computer Methods in Applied Mechanics and Engineering* 2001; **190**(49-50):6577-6604.

4. Yin Luzhong, Anathasuresh GK. A novel topology design scheme for the multiphysics problems of electro-thermally actuated compliant micromechanisms. *Sensors and Actuators A* 2002; **97-98**:599-609.

5. Sigmund O, Jensen JS. Systematic design of phononic band gap materials and structures by topology optimization. *Philosophical transactions of the royal society A: Mathematical, Physical and Engineering Sciences* 2003; **361**:1001-1019.

6. Yoon GH, Kim YY. The element connectivity parameterization formulation for the topology design optimization of multiphysics systems. *International Journal for Numerical Methods in Engineering* 2005; 64:1649-1677.

7. Sigmund O., Clausen PM. Topology optimization using a mixed formulation : An alternative way to solve pressure load problems. Submitted.

8. Hammer VB, Olhoff N. Topology optimization of continuum structures subjected to pressure loading. *Structural and Multidisciplinary Optimization* 2000; **19**: 85-92.

9. M. Raulli, K. Maute. Topology optimization of electrostatically actuated microsystems. *Structural and Multidisciplinary Optimization* 2005; **30**(5): 342-359.

10. Marburg S, Beer HJ, Gier J, Hardtke HJ. Experimental verification of structural acoustic modelling and design optimization. *Journal of Sound and Vibration* 2002; **252(4)**:591-615.

11. Lee JW, Wang SM. Shape design sensitivity analysis for the radiated noise from the thin-body. *Journal of Sound and Vibration* 2003; **261**: 895-910.

12. Luo J, Gea HC. Optimal stiffener design for interior sound reduction using a topology optimization based approach. *Journal of Vibration and acoustics* 2003; **125**: 267-273.

13. Lee JW, Wang SM, Dikec A. Topology optimization for the radiation and scattering of sound from thin-body using genetic algorithms. *Journal of Sound and Vibration* 2004; **276**: 899-918.

14. Jog CS. Reducing radiated sound power by minimizing the dynamic compliance. Proc. IUTAM Conference on Design for Quietness, Kluwer Academicpt Publishers, 2002.

15. Olhoff N, Du J. Topological design for minimum dynamic compliance of continuum structures subjected to forced vibration. *Structural and Multidisciplinary Optimization* 2005, submitted.

16. Chang YC, Yeh LJ, Chiu MC. Optimization of double-layer absorbers on constrained sound absorption system by using genetic algorithm. *International Journal for Numerical Methods in Engineering* 2005; **62**:317-333.

17. Allen M, Maute K. Reliability-based shape optimization of structures undergoing fluid-structure interaction phenomena. *Computer Methods in Applied Mechanics and Engineering* 2005; **194**: 3472-3495.

18. Divo EA, Kassab AJ, Ingber MS. Shape optimization of acoustic scattering bodies. *Engineering Analysis with Boundary Elements* 2003; **27**: 695-703.

19. Meric RA. Shape design sensitivity analysis and optimization for the non-homogeneous Helmholtz equation by the bem. *Communications in Numerical Methods in Engineering* 1996; **12**: 95-105.

20. Dong J, Choi KK, Wang A, Zhang W, Vlahopoulos N. Parametric design sensitivity analysis of high-frequency structural-acoustic problems using energy finite element method. *International Journal for Numerical Methods in Engineering* 2005; **62**:83-121.

21. Marburg S, Hardtke HJ. Shape optimization of a vehicle hat-shelf improving acoustic properties for different load cases by maximizing first eigenfrequency. *Computers and Structures* 2001; **79**:1943-1957.

22. Bathe KJ, Zhang H. Finite element developments for general fluid flows with structural interaction. *International Journal for Numerical Methods in Engineering* 2004; **60**:213-232.

23. Greenshields CJ, Weller HG. A unified formulation for continuum mechanics applied to fluid-structure interaction in flexible tubes. *International Journal for Numerical Methods in Engineering* In press.

24. Wang X, Bathe KJ. Displacement/pressure based mixed finite element formulations for acoustic fluid-structure interaction problems. *International Journal for Numerical Methods in Engineering* 1997; **40**:2001-2017.

25. Bängtsson E, Noreland D, Berggren M. Shape optimization of an acoustic horn. *Computer Methods in Applied Mechanics and Engineering* 2003; **192**: 1533-1571.

26. Soize C, Michelucci JC. Structural shape parametric optimization for an internal structural-acoustic problem. *Aerosp. Sci. Technol.* 2000; **4**:263-275.

27. Junhong Z, Jun H. CAE process to simulate and optimize engine noise and vibration. *Mechanical*

Systems and Signal Processing In press.

28. Bathe KJ. *Finite element procedures*. Prentice hall: New Jersey, 1996.

29. Allaire G, Jouve F, Toader AM. Structural optimization using sensitivity analysis and a level-set method. *Journal of Computational Physics* 2004; **194(1)**:363-393.

30. Chang YC, Yeh LJ, Chiu MC. Optimization of double-layer absorbers on constrained sound absorption system by using genetic algorithm. *International Journal for Numerical Methods in Engineering* 2005; **62**:317-333.

31. Kinsler LE, Frey AR, Coppens AB, Sanders JV. *Fundamentals of acoustics*. John Wiley& Sons, Inc.: USA, 2000.

32. N. L. Pedersen. Maximization of eigenvalues using topology optimization. *Structural and Multidisciplinary Optimization* 2000; **20(1)**: 2-11.

33. Sigmund O, Torquato S. Design of materials with extreme thermal expansion using a three-phase topology optimization. *Journal of the Mechanics and Physics of Solids* 1997; **45(6)**: 1037-1067.

34. Bendsøe MP, Sigmund O. Material interpolation schemes in topology optimization. *Archives of Applied Mechanics* 1999; **69(9-10)**: 635-654.

35. Olesen LH, Okkels F, Bruus H. A high-level programming-language implementation of topology optimization applied to steady-state Navier-Stokes flow. *International Journal for Numerical Methods in Engineering,* 2006; **65(7)**: 975-1001.

36. Liu Z, Korvink JG, Huang R. Structure topology optimization: fully coupled level set method via FEMLAB. *Structural and Multidisciplinary Optimization* 2005; **29(6)**: 407-417.

37. Gersborg-Hansen A, Sigmund O, Harber RB. Topology optimization of channel flow-problems. *Structural and Multidisciplinary Optimization* 2005; **30(3)**: 181-192.

38. Svanberg K. The method of moving asymptotes - a new method for structural optimization. *International Journal for Numerical Methods in Engineering* 1987; **24**:359-373.

39. Yoon GH, Kim YY. Optimal design of the optical pickup suspension plates using topology optimization. AIAA 2003; 1841-1843.